# Simple Model to Predict Gel Formation in Olefin-Diene Copolymerizations Catalyzed by Constrained-Geometry Complexes

**Job D. Guzmán, Daniel J. Arriola, Teresa Karjala, Joshua Gaubert, and Brian W. S. Kolthammer**
The Dow Chemical Company, Freeport, TX 77541

*DOI 10.1002/aic.12057*
*Published online October 22, 2009 in Wiley InterScience (www.interscience.wiley.com).*

*We have developed an analytical model to predict the onset of gel formation in ethylene/1-octene/1,9-decadiene terpolymerizations using constrained-geometry catalysts. The model relies on three kinetic parameters to characterize the catalyst response. Polymer resins have been synthesized in a continuous stirred-tank reactor to determine the model parameters, and to validate the model predictions for polymer properties and for the onset of gel formation and reactor fouling. The experimental results indicate that the free double bonds in 1,9-decadiene are as reactive as those found in 1-octene, and that the reactivity of 1,9-decadiene double bonds decreases after the 1,9-decadiene molecules become part of a polymer chain. The model predictions of polymer properties agree well with chromatographic, density, and mass-balance data. Moreover, the model was successful in preventing unintended reactor fouling during the duration of the experimental campaign.* © 2009 American Institute of Chemical Engineers *AIChE J,* 56: 1325–1333, 2010
*Keywords: polymerization, mathematical modeling, reaction kinetics, process control*

## Introduction

Adding a few long branches to otherwise linear polymer chains improves the rheological behavior of the polymer system. At low shear rates, sparse long-chain branching (LCB) increases the resins' viscosity,[1] because long-chain branches hinder polymer chain movement when they become entangled. At high shear rates, the branch entanglements relax and resins with LCB display more shear thinning than their linear counterparts.[2] Long chain branching also increases the resins'- elasticity,[2] melt strength,[3] and fiber-spinning stability.[4] Therefore, long-chain-branched resins can provide both the desirable hardness in the final product and the convenience of fast flows during polymer processing.

Polyethylene resins made with Constrained-Geometry Catalysts (CGCs) contain long-chain branches, because the exposed-metal structure found in CGCs permits the incorporation of macromonomers into the growing polymer chain.[5] Macromonomers are generated in situ when a reactive double bond is formed in a polymer chain via $\beta$-hydride elimination. $\beta$-hydride elimination, however, produces macromonomers with only one reactive double bond per molecule, and the resulting LCB levels in CGC resins are relatively low.[6]

Copolymerization with linear unconjugated dienes is one way to significantly increase LCB levels in CGC resins, opening possibilities for the development of new products with improved processability and optimal mechanical properties. Figure 1 illustrates the chemical structures expected in CGC ethylene-diene copolymerizations. Dienes produce LCB because the incorporation of dienes into growing polymer chains produces dangling vinyl groups; these unreacted vinyl groups offer additional branching points, and they increase the likelihood of LCB reactions. Not all dienes, however, are equally effective in inducing LCB. 1,5-hexadiene, for instance, mainly forms five-member rings along the polymer chains, and it does not produce any significant amount of *H* branches coupling two polymer chains.[7] Longer

Correspondence concerning this article should be addressed to J. D. Guzmán at job.guzman@dow.com

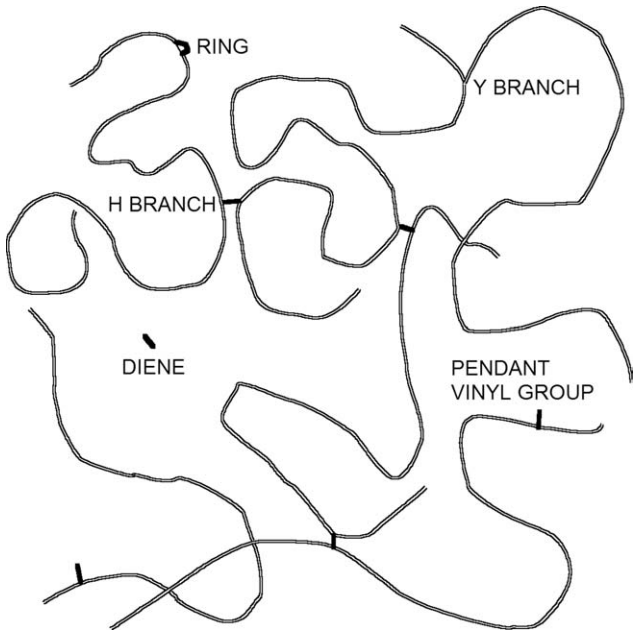


**Figure 1. Chemical structures in CGC ethylene-diene copolymerizations.**

dienes are less susceptible to cyclization. 1,9-decadiene in particular produces long-chain branches without forming any cycles within nuclear-magnetic-resonance (NMR) detection capabilities.[8]

The LCB efficiency of a diene molecule is also affected by the relative reactivity of the two double bonds in the diene. The double bonds attached to polymer chains are less reactive than the double bonds in unattached diene molecules,[9] presumably because of steric hindrance. When there are significant differences in reactivity, branching reactions do not occur until most of the diene molecules are incorporated in the polymer, and no branching is detected if the polymerization is stopped too soon.[8] Marked differences in reactivity pose control problems in the manufacturing of branched resins. When branching reactions occur only after most of the branching points have already been created, branching occurs in mass, and gelation occurs rapidly without much warning.

Excessive crosslinking of the polyethylene resin affects the product quality, and it can lead to severe fouling of commercial reactors. To control LCB and to avoid gelation, the polymerization engineer must know (a priori) the amount of diene leading to gel formation. Simple rules of thumb, such as not exceeding 2000 ppm of diene, are inappropriate, because 2000 ppm can be either too much or too little diene, depending on the reactor conditions and the product-property targets. The critical diene concentration leading to gelation varies depending on the feed composition, the ethylene conversion, the degree of polymerization, the catalyst behavior, and the reactor residence time. The goal of this work is to develop a simple model to predict the critical diene concentration for gelation as function of reaction conditions for well-mixed, continuous systems. In addition, the model should provide accurate estimates of the polymer molecular weight and polydispersity for a given diene concentration to help meet product specifications in continuous, commercial reactors.

Previous modeling studies of olefin-diene copolymerizations have typically focused on semi-batch systems, and they have used finite element[10] or generating functions[11] to address the numerical complexities encountered in rigorous non-linear polymerization modeling. Here, we have made several simplifications to derive a simple analytical relation suitable for process control of industrial reactors. The relation given here is directly applicable to continuous polymerizations, which are known to display different critical concentrations than their batch counterparts.[12,13] Moreover, unlike previous modeling studies, we make quantitative comparisons between modeling predictions and experimental data, and we show how the model can be used to prevent reactor fouling.

### *Modeling*

Following ver Strate et al.,[12] we start by considering the simplified set of reactions given in Table 1, where $[P_i]$ and $[Q_i]$ are the concentrations of growing and terminated polymer chains with $i$ repeat units, and $[M]$ is the monomer concentration. The rate of coupling is proportional to the length ($j$) of the terminated chain, because the number of branching points (pendant vinyl groups) increases with increasing chain length. The Strate et al. kinetic scheme was originally developed for free-radical polymerization, but the differences between termination mechanisms in free-radical and transition-metal polymerizations do not change the predictions for gelation.

Material balances for $[P_i]$, $[Q_i]$, and $[M]$ in a perfectly-mixed continuous stirred-tank reactor (CSTR) are given by ver Strate et al. It is assumed that the mean life time of growing chains is very short ($[P] \ll [Q]$), that all coupling reactions are intermolecular, and that depletion of enchained double bonds after a chain coupling is negligible. Upon integration of the $[P_i]$ and $[Q_i]$ material balances by the method of moments, ver Strate et al.[12] derive the following relations:

$$h_{\text{crit}} = 1/(4 \times \text{DP}_{\text{w}}^0), \tag{1}$$

$$\text{DP}_{\text{n}} = \text{DP}_{\text{n}}^0/(1 - h \times \text{DP}_{\text{n}}^0), \tag{2}$$

$$\text{DP}_{\text{w}} = \text{DP}_{\text{w}}^0(1 + h \times \text{DP}_{\text{w}})^2. \tag{3}$$

where, $\text{DP}_{\text{n}}$ and $\text{DP}_{\text{w}}$ are the number- and weight average degrees of polymerization for the branched polymer, and $\text{DP}_{\text{n}}^0$ and $\text{DP}_{\text{w}}^0$ are the corresponding degrees of polymerization for the linear backbone. $h$ is the average mole fraction of H branches present in the polymer, and $h_{\text{crit}}$ is the value of $h$ where gelation occurs.

**Table 1. Polymerization Reactions**

| Step | Reaction | Rate |
|---|---|---|
| Propagation | $P_i + M \rightarrow P_{i+1}$ | $k_{\text{P}}\,[M][P_i]$ |
| Termination | $P_i \rightarrow Q_i$ | $k_{\text{T}}\,[P_i]$ |
| Coupling | $P_i + Q_j \rightarrow P_{i+j}$ | $k_{\text{C}}\,j[P_i\,][Q_j]$ |

The quantities $k_{\text{P}}$, $k_{\text{T}}$, and $k_{\text{C}}$ are, respectively, the main monomer propagation rate constant, the termination rate constant, and an overall rate parameter describing the reactivity of a random polymer repeat unit.

**Table 2. Diene Reactions**

| Step | Reaction | Rate |
|---|---|---|
| Vinyl formation | $P + D_2 \rightarrow D_1$ | $k_V\,[D_2][P]$ |
| $H$ branch formation | $P + D_1 \rightarrow D_0$ | $k_H\,[D_1][P]$ |

$k_V$ is the propagation rate constant of the free diene, and $k_H$ a formal coupling rate constant replacing $k_C$, the rate parameter used by ver Strate.[13]

Since the model does not include any dynamic effects, $h_{crit}$ indicates the degree of crosslinking leading to gel formation at steady state. For $h \geq h_{crit}$, the reactor reaches a steady state with a stable gel fraction when the amount of gel produced is balanced by the amount of gel leaving the reactor.[13] In practice, a steady state may be difficult to achieve when $h \geq h_{crit}$, because of gel accumulation inside the reactor and polymer fouling.

The Strate et al. equations can be expressed in terms of a normalized degree of crosslinking

$$X = h/h_{crit}. \tag{4}$$

For instance,

$$\frac{M_w}{M_w^0} = \frac{DP_w}{DP_w^0} = 8\frac{1 - X/2 - \sqrt{1-X}}{X^2}. \tag{5}$$

Equation 5 indicates that the weight-average molecular weight of a linear polymer $M_w^0$ can only be increased by a factor of four in extreme conditions (operating at the onset of gelation). Similarly, assuming that $DP_w^0 = 2 \times DP_n^0$, the polydispersity index (PDI) of the branched polymer is given by

$$PDI = \frac{DP_w}{DP_n} = \frac{(X + 2\sqrt{1-X} - 2)(X-8)}{X^2}, \tag{6}$$

indicating that the maximum pre-gel PDI at steady state is seven. Equation 6 can be inverted to estimate the degree of crosslinking of a decadiene copolymer sample from its PDI, i.e.,

$$X = 2\frac{4 + \left(\sqrt{8PDI - 7} - 5\right)PDI}{(PDI - 1)^2}. \tag{7}$$

Simple correction factors in Eqs. 6 and 7 are used to recognize that the PDI*s* of CGC resins are typically slightly greater than two in the absence of decadiene.

To relate the fraction of crosslinks ($h$) to the decadiene concentration, we consider the reactions given in Table 2, where the quantity $D_2$ represents an unattached decadiene molecule, $D_1$ is a pendant vinyl group (attached to a polymer chain), and $D_0$ is an $H$ branch coupling two polymer chains. Cyclization reactions are neglected because, as confirmed by our own NMR measurements, decadiene does not appear to form any rings on the polymer chains.

On the basis of Table 2, a decadiene mass balance in a CSTR at steady state leads to

$$[D_2] = C_0 - 2[D_2]Da, \tag{8}$$

$$[D_1] = 2[D_2]Da - [D_1]Da/r \tag{9}$$

$$[D_0] = [D_1]Da/r \tag{10}$$

where, the feed concentration $C_0$ is equal to the total mole concentration of decadiene moieties in the reactor ($C_0 = [D_2] + [D_1] + [D_0]$), $Da$ is the Damköhler number for a given residence time ($Da = \tau\, k_V[P]$), and $r$ is the ratio of the diene reaction rate constants; i.e., $r = k_V/k_H$. The factor of 2 in Eqs. 8 and 9 is needed because there are two indistinguishable reactions involving unattached decadiene molecules.

With decadiene conversion (for the entire molecule) defined as

$$x_3 = \frac{C_0 - [D_2]}{C_0}, \tag{11}$$

the last four equations (Eqs. 8–11) are rearranged to express four variables: $[D_2]$, $[D_1]$, $[D_0]$, and $Da$ as a function of $x_3$, $r$, and $C_0$; for instance:

$$[D_0] = \frac{C_0 x_3^2}{x_3 + 2r(1 - x_3)} \text{ and} \tag{12}$$

$$[D_1] = \frac{2C_0 r x_3 (1 - x_3)}{x_3 + 2r(1 - x_3)}. \tag{13}$$

The mole fraction of $H$ branches present in the polymer is

$$h = F \times [D_0]/P_R, \tag{14}$$

where, $F$ is the total molar feed flow (including solvent), and $P_R$ is the molar production rate: $P_R = \sum F_i x_i$, where $F_i$ and $x_i$ are, respectively, the inlet molar flow and the conversion for monomer $i$, and the sum includes all the monomers involved in the polymerization. The critical decadiene feed concentration for gelation is obtained by equating Eq. 14 to Eq. 1; i.e.,

$$\tilde{C}_{0,crit} = \frac{(x_3 + 2r(1 - x_3))P_R}{4\tilde{F}\, DP_w^0 x_3^2} \times M_{DD} \times 10^6. \tag{15}$$

where, $\tilde{C}_{0,crit}$ is the critical decadiene feed concentration in weight parts per million, $\tilde{F}$ is the total mass feed flow, and $M_{DD}$ is the molecular weight of decadiene (138.26 g/mol). Equation 15 is the most important equation is this publication. It defines the (variable) gelation boundary, and it should help prevent unintentional synthesis of macroscopic polymer networks in olefin-diene copolymerizations. The normalized degree of crosslinking, needed to estimate molecular weight and polydispersity (via Eqs. 5 and 6), is given by:

$$X = \tilde{C}_0/\tilde{C}_{0,crit}, \tag{16}$$

where, $\tilde{C}_0$ is the decadiene feed concentration in weight ppm (any self-consistent concentration units can be used in Eq. 16).

The decadiene conversion (needed in Eq. 15) is related to the ethylene conversion via copolymerization kinetics. In general, for the copolymerization of two monomers "1" and "2", the instantaneous copolymer composition is related to

the reactor monomer composition by the Mayo-Lewis equation.[14]:

$$\dot{F}_1 = \frac{r_{12}f_1^2 + f_1 f_2}{r_{12}f_1^2 + 2f_1 f_2 + r_{21}f_2^2}. \quad (17)$$

where, $\dot{F}_1$ is mole fraction of monomer "1" in the polymer chain, $f_1$ and $f_2$ are the molar monomer fractions in the reactor monomer mixture ($f_1 + f_2 = 1$), and $r_{12}$ and $r_{21}$ are the copolymerization reactivity ratios. That is, $r_{ij} = k_{ii}/k_{ij}$, where $k_{ij}$ is the reaction rate constant for the addition of monomer $j$ to a polymer chain terminated in monomer $i$.

In a single, well-mixed CSTR, the instantaneous copolymer composition ($\dot{F}_i$) and the steady-state copolymer composition are one and the same. Thus, Eq. 17 (developed initially for batch reactors) is directly applicable to CSTRs. Moreover, our internal studies indicate that the CGC system used here produces nearly random ethylene-octene copolymers; i.e., when "1" denotes ethylene and "2" octene, $r_{12} \times r_{21} \approx 1$. The same relation between reactivity ratios has been reported in other copolymerization studies using CGC systems.[15–17] When $r_{12} \times r_{21} = 1$, Eq. 17 reduces to

$$x_2 = \frac{x_1}{x_1 + r_{12} - x_1 r_{12}}, \quad (18)$$

where from now on "1" and "2" denote ethylene and octene, and $x_1$ and $x_2$ are, respectively, the ethylene and octene conversions. Assuming CGC ethylene-decadiene copolymerizations are also random,

$$x_3 = \frac{x_1}{x_1 + r_{13} - x_1 r_{13}}, \quad (19)$$

where "3" denotes decadiene and $r_{13} = k_{11}/k_{13} \approx k_P/k_V$. Note that because $x_3$ is the conversion for entire decadiene molecule, $1/r_{13}$ indicates the combined reactivity of the two double bonds in the diene.

For terpolymers made of ethylene, 1-octene, and 1,9-decadiene, a rigorous analysis requires six reactivity ratios: $r_{12}$, $r_{13}$, $r_{21}$, $r_{23}$, $r_{31}$, and $r_{32}$. The addition of minute quantities of a third monomer, however, is not expected to disrupt the random copolymerization behavior of the ethylene-octene system. For a random terpolymerization where $r_{ij} = 1/r_{ji}$, there are only three independent reactivity ratios; e.g., $r_{12}$, $r_{13}$, and $r_{32}$. Further, since only minute quantities of decadiene are present, the addition of decadiene molecules to decadiene-terminated polymer chains is highly unlikely; our experimental data does not contain information on the value of $k_{33}$, and fitting $r_{32} = k_{33}/k_{32}$ to our data is unwarranted. The related ratio $r_{23} = k_{22}/k_{23}$ is somewhat more relevant than $r_{32}$, but the accurate determination of $r_{23}$ is also problematic, given the experimental difficulties associated with tracking minute concentrations of decadiene molecules along the polymer chain.

In this work, we have assumed that the terpolymerization is well described by two reactivity ratios ($r_{12}$ and $r_{13}$), and that this two reactivity ratios are related to octene and decadiene conversion according to Eqs. 18 and 19, respectively. To the extent that reactions between decadiene and octene terminal groups occur, the reactivity ratios determined from Eqs. 18 and 19 are lumped kinetic parameters including major and minor reactions.

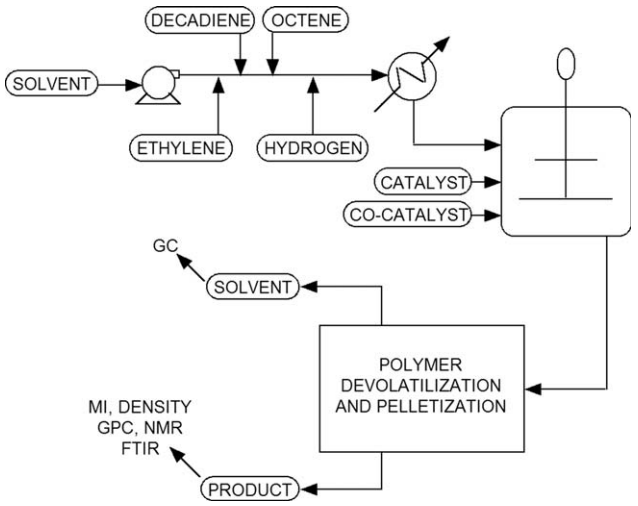


**Figure 2. Continuous process for the synthesis of ethylene/1-octene/1,9-decadiene terpolymers.**

## Experimental

To determine the three kinetic parameters ($r_{12}$, $r_{13}$, $r$) for the CGC system, we have synthesized 25 resins at different reactor conditions, and we have characterized the molecular weight and microstructure of each resin.

Figure 2 illustrates the continuous process used to synthesize the resins. Purified reactants are mixed with cold solvent before entering the reactor. Catalyst and co-catalyst are injected separately. The 1-gallon reactor is maintained at constant pressure and temperature. Two impellers, rotating at typical speeds of 1000 rpm, homogenize the reactor liquor with four stationary stiffeners supporting the agitator assembly acting as anti-vortex baffles. The polymer solution exiting the reactor is heated and then flashed to separate the polymer product from the solvent. Monomer conversion is determined from the composition of the spent solvent, which is measured via gas chromatography. There is no recirculation of solvent or unreacted monomer.

Table 3 lists the 25 experimental runs. Before letting decadiene into the reactor, the product melt index was set to a desired value by manipulating the inlet flow of hydrogen (a chain transfer agent that increases termination reactions). Once the required hydrogen flow for a given melt index was established, the hydrogen flow rate was kept constant when decadiene was entering the reactor, and sufficient time was allowed for a new melt index to be established. At all times, ethylene conversion was kept at a desired value by manipulating the inlet flow of catalyst. Since the required flow rates of hydrogen and catalyst are relatively small, significant changes in the product molecular weight and in the ethylene conversion can be attained without changing the reactor residence time, which was kept fairly constant during all runs.

In runs 1 through 12, only ethylene and 1,9-decadiene were copolymerized. In runs 13 through 25, a terpolymer of ethylene, 1-octene, and 1,9-decadiene was synthesized. Reactor fouling was studied in runs 19 through 25. To verify the

**Table 3. Reactor Conditions**

| Sample | $C_2$ feed (wt%) | $C_8$ feed (wt%) | $C_{10}$ feed (ppm) | $I_2^0$, dg/min | $C_2$ % Conversion | Production rate, kg/h |
|---|---|---|---|---|---|---|
| 1 | 15.4 | 0.0 | 0 | 20.0 | 79 | 2.2 |
| 2 | 15.4 | 0.0 | 521 | 19.5 | 79 | 2.2 |
| 3 | 15.4 | 0.0 | 0 | 19.0 | 79 | 2.2 |
| 4 | 15.4 | 0.0 | 0 | 4.9 | 80 | 2.3 |
| 5 | 15.4 | 0.0 | 284 | 4.5 | 80 | 2.3 |
| 6 | 15.4 | 0.0 | 0 | 4.0 | 80 | 2.3 |
| 7 | 13.6 | 0.0 | 0 | 5.1 | 90 | 2.3 |
| 8 | 13.6 | 0.0 | 131 | 5.0 | 89 | 2.3 |
| 9 | 13.6 | 0.0 | 0 | 5.0 | 90 | 2.3 |
| 10 | 13.6 | 0.0 | 0 | 21.5 | 89 | 2.2 |
| 11 | 13.6 | 0.0 | 196 | 19.1 | 90 | 2.3 |
| 12 | 13.6 | 0.0 | 0 | 16.7 | 89 | 2.3 |
| 13 | 10.0 | 12.9 | 0 | 15.0 | 79 | 2.3 |
| 14 | 10.0 | 12.9 | 285 | 13.5 | 79 | 2.3 |
| 15 | 10.0 | 12.9 | 0 | 12.0 | 78 | 2.2 |
| 16 | 12.4 | 2.1 | 0 | 5.3 | 90 | 2.3 |
| 17 | 12.5 | 2.1 | 140 | 5.2 | 90 | 2.3 |
| 18 | 12.4 | 2.1 | 0 | 5.1 | 90 | 2.3 |
| 19 | 13.9 | 3.6 | 0 | 20.0 | 79 | 2.2 |
| 20 | 13.9 | 3.6 | 523 | 20.0 | 79 | 2.2 |
| 21 | 13.9 | 3.6 | 704 | 20.0 | 79 | 2.2 |
| 22 | 13.9 | 3.6 | 794 | 20.0 | 79 | 2.2 |
| 23 | 13.9 | 3.6 | 837 | 20.0 | 79 | 2.2 |
| 24 | 13.9 | 3.6 | 881 | 20.0 | 79 | 2.2 |
| 25 | 13.9 | 3.6 | 923 | 20.0 | 79 | 2.2 |

All runs were conducted at 155°C. The bulk of the feed flow is solvent; small concentrations of catalyst and hydrogen are also present. $C_2$, $C_8$, and $C_{10}$ stand for ethylene, 1-octene, and 1,9-decadiene. $I_2^0$ stands for the polymer melt index in the absence of $C_{10}$. $I_2^0$ is controlled to a desired value by manipulating the inlet flow of hydrogen. The ethylene conversion is controlled by the flow of catalyst.

theoretical predictions for gelation and their relation to actual fouling, all variables were kept constant while an ever increasing amount of decadiene was fed to the reactor. Monitoring the process for signs of fouling was particularly important during the last runs, to stop the decadiene feed before causing massive fouling. An increase in the feed pressure suggests injector plugging. Discrepancies among the four temperature sensors, vertically stacked along the reactor wall, indicate possible polymer buildup on the thermocouples. A gradual opening of the reactor pressure-control valve, under otherwise steady-state operating conditions, signals a possible restriction in the piping downstream of the reactor. Note that the formation of polymer gels is only one of the possible causes for polymer fouling. Fouling can also occur after the precipitation of highly crystalline polymer chains in cold spots, or after the precipitation of very high molecular weight linear chains.

The polymer products were characterized via melt index and density measurements, NMR imaging, Fourier-transform infrared (FTIR) spectroscopy, and triple-detection gel-permeation-chromatography (TD-GPC) analyses.

The melt index values, $I_2$ and $I_{10}$, were measured according to ASTM D-1238. The value of $I_2$ correlates with the molecular weight of the resin. An increase in the $I_{10}/I_2$ ratio indicates enhanced shear thinning, and it is evidence of LCB reactions. The polymer density, a proxy for octene incorporation, was measured according to ASTM D-792. NMR imaging was used to detect cyclic groups with a Varian 500 MHz spectrometer. No cyclic groups were found in any of the samples. FTIR spectroscopy was used to measure the concentration of vinyl groups, according to ASTM D-3124 using a Thermo Nicolet Nexus 470.

The TD-GPC system consisted of a Waters high-temperature chromatograph equipped with a laser light-scattering detector, an infra-red detector, and a capillary viscometer. The GPC column set was calibrated with 21 narrow-molecular-weight-distribution polystyrene standards from Polymer-Laboratories, and the measurements were converted to polyethylene molecular weights using a standard procedure.[18] For each analysis, 0.1 g of polymer were dissolved in 50 milliliters of 1,2,4-trichlorobenzene, by gently stirring at 160°C for 4 hr. An injection volume of 200 $\mu$l and a flow rate of 1 ml/min were used. The carousel was operated at 140°C, the columns at 150°C.

## Results and Discussion

Table 4 indicates the melt index, the density, the weight-average molecular weight ($M_w$), the polydispersity, and the vinyl and decadiene content for each sample. Density, $M_w$, and decadiene content data are used to determine kinetic parameters. The model is then used to calculate the polydispersity and the vinyl content of the resins, and to predict the onset of fouling.

The simultaneous fitting of the three kinetic parameters to the data shown in Table 4 is a non-linear optimization problem with multiple solutions. To obtain a single solution, we fit kinetic parameters one at a time to key data. First, $r_{12}$ is fitted to density measurements, because the density of the polymer is determined by its octene composition and the effect of other kinetic parameters on density is minimal. Next, $r_{13}$ is fitted to decadiene polymer composition data (relating decadiene reactivity with decadiene incorporation), and lastly $r$ is fitted to molecular-weight measurements, matching the decadiene LCB efficiency with the observed increased in $M_w$. The $r_{12}$, $r_{13}$, and $r$ values obtained in this sequential procedure establish an unambiguous "initial guess" for simultaneous numerical optimization, if improvements to the fit are necessary.

Figure 3 illustrates the determination of $r_{12}$. For a given value of $r_{12}$, octene conversion is calculated from Eq. 18, the octene polymer composition is calculated from a mass balance, and the density is estimated from an empirical correlation (relating density to octene content). The value of $r_{12}$ that best fits the density data is roughly 7.5.

Figure 4 illustrates the determination of $r_{13}$. The decadiene conversion is calculated from Eq. 19, and the decadiene polymer composition is calculated from a mass balance. The value of $r_{13}$ that best fits the polymer composition data is $\sim$3.75, half the value of $r_{12}$, indicating that decadiene is twice as reactive as octene. The increase in reactivity is expected, as the decadiene molecule has two double bonds. That $r_{12} = 2 \times r_{13}$ indicates that each unattached decadiene double bond is as reactive as the octene double bond.

In Figure 5, we compare the model predictions for the fractional increase in molecular weight caused by decadiene crosslinks ($M_w/M_w^0$) with the corresponding TD-GPC measurements. The value of $r$ that best fits the molecular-increase data is 2.85, a relatively high value, indicating that

**Table 4. Experimental Results**

| Sample | $I_2$, dg/min | $I_{10}/I_2$ | $\rho$, g/cm$^3$ | $M_W^0$, kg/mol | $M_W$, kg/mol | PDI | Vinyls/1000 C | $C_{10}$ inc. (ppm) |
|---|---|---|---|---|---|---|---|---|
| 1 | 20.0 | 5.9 | 0.964 | 48 | 48 | 2.3 | 0.12 | 0 |
| 2 | 4.2 | 10.2 | 0.959 | 48 | 62 | 2.8 | 0.25 | 2048 |
| 3 | 19.0 | 6.4 | 0.963 | | | | | 0 |
| 4 | 4.9 | 7.0 | 0.959 | 64 | 64 | 2.4 | 0.09 | 0 |
| 5 | 1.0 | 12.6 | 0.956 | 65 | 82 | 3.0 | 0.13 | 1223 |
| 6 | 4.0 | 6.9 | 0.959 | 67 | 67 | 2.4 | 0.06 | 0 |
| 7 | 5.1 | 7.4 | 0.960 | 61 | 61 | 2.4 | 0.08 | 0 |
| 8 | 1.8 | 11.1 | 0.958 | 61 | 71 | 2.7 | 0.09 | 669 |
| 9 | 5.0 | 8.0 | 0.960 | | | | | 0 |
| 10 | 21.5 | 6.5 | 0.963 | 44 | 44 | 2.3 | 0.11 | 0 |
| 11 | 5.5 | 9.4 | 0.961 | 45 | 57 | 2.7 | 0.14 | 1021 |
| 12 | 16.7 | 6.7 | 0.961 | 47 | 47 | 2.4 | 0.11 | 0 |
| 13 | 15.0 | 7.9 | 0.875 | 67 | 67 | 3.0 | 0.15 | 0 |
| 14 | 9.3 | 9.8 | 0.874 | 69 | 82 | 3.5 | 0.22 | 1316 |
| 15 | 12.0 | 8.1 | 0.876 | 71 | 71 | 2.7 | 0.14 | 0 |
| 16 | 5.3 | 7.6 | 0.922 | 62 | 62 | 2.4 | 0.10 | 0 |
| 17 | 2.0 | 10.7 | 0.922 | 62 | 76 | 2.7 | 0.15 | 716 |
| 18 | 5.1 | 7.6 | 0.922 | 63 | 63 | 2.8 | 0.11 | 0 |
| 19 | 20.0 | 6.2 | 0.921 | 48 | 48 | 2.2 | 0.11 | 0 |
| 20 | 7.2 | 9.1 | 0.922 | 48 | 59 | 2.9 | 0.25 | 2119 |
| 21 | 4.6 | 10.2 | 0.923 | 48 | 67 | 3.1 | 0.29 | 2912 |
| 22 | 3.2 | 11.0 | 0.922 | 48 | 74 | 3.3 | 0.30 | 3186 |
| 23 | 3.1 | 11.5 | 0.922 | 48 | 75 | 3.5 | 0.30 | 3405 |
| 24 | 2.1 | 11.8 | 0.922 | 48 | 82 | 3.5 | 0.28 | 3502 |
| 25 | 1.3 | 13.0 | 0.922 | 48 | 90 | 3.8 | 0.31 | 3946 |

The indicated PDI was determined via TD-GPC. $C_{10}$ inc. is the weight fraction of the polymer chain that is made of decadiene molecules, according to decadiene mass balance measurements.

unattached double bonds are almost three times more reactive than their enchained counterparts.

The model developed here is tested by comparing its predictions with experimental data, not used in the fitting of the kinetic parameters. Figure 6 shows the model predictions for PDI values along with the corresponding GPC measurements, as a function of the normalized degree of crosslinking ($X$). The agreement with TD-GPC data is satisfactory, especially for samples with relatively high $X$ values where decadiene crosslinks are more abundant than "$Y$" long-chain

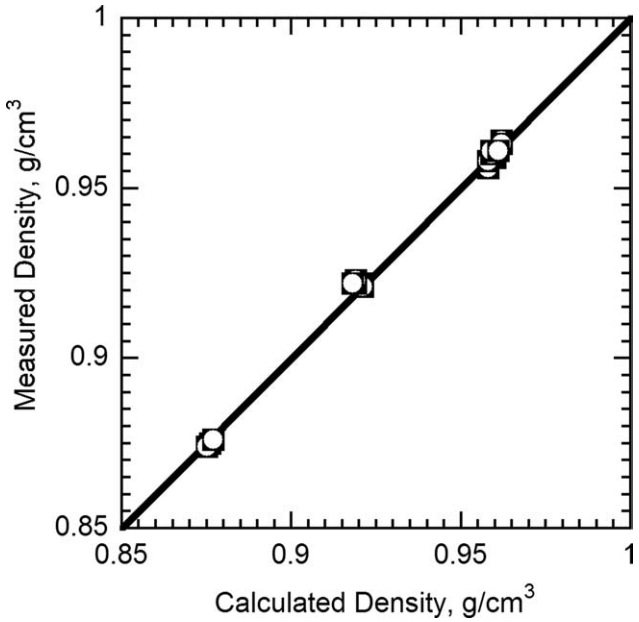


**Figure 3. Determination of $r_{12}$.**

Line: best possible agreement between experimental measurements and model predications. Points' $x$ coordinates: calculated density values using $r_{12} = 7.5$, and data from Table 3. Points' $y$ coordinates: experimental measurements from Table 4.

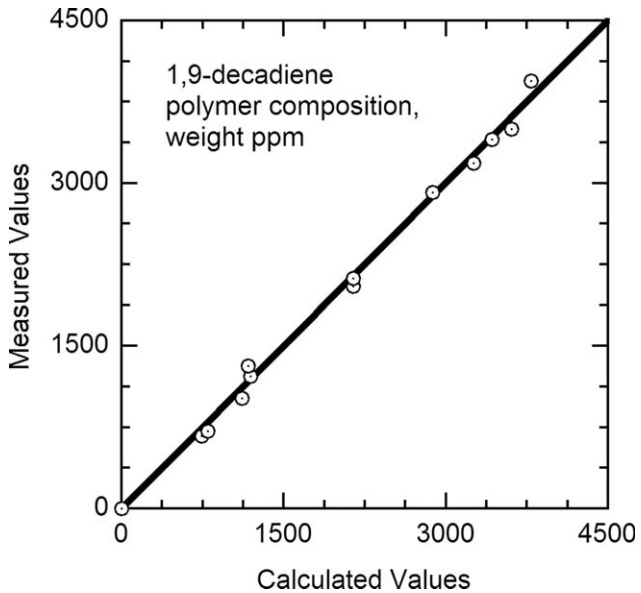


**Figure 4. Determination of $r_{13}$.**

Line: best possible agreement between experimental measurements and model predications. Points' $x$ coordinates: calculated decadiene polymer composition using $r_{13} = 3.75$, $r_{12} = 7.5$, and data from Table 3. Points' $y$ coordinates: experimental measurements from Table 4.

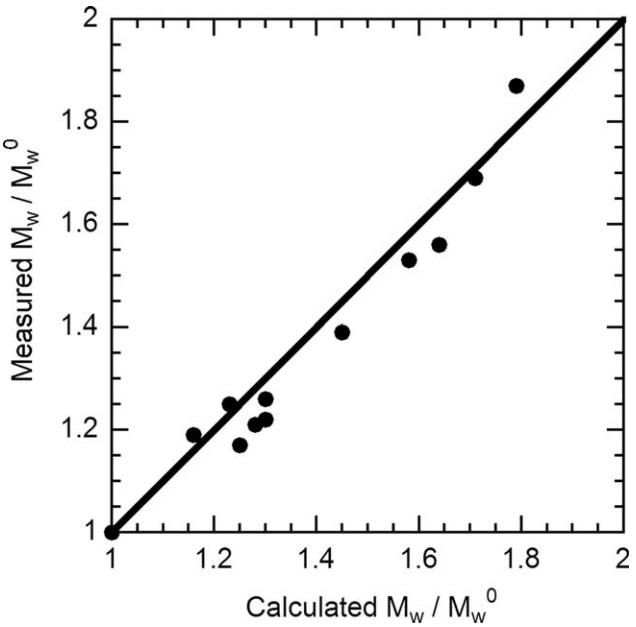


**Figure 5. Determination of *r*.**

Line: best possible agreement between experimental measurements and model predications. Points' $x$ coordinates: calculated values via Eq. 5 using $r = 2.85$, $r_{13} = 3.75$, $r_{12} = 7.5$, and input data from Table 3. Points' $y$ coordinates: TD-GPC measurements of the fractional increase in molecular weight (Table 4).

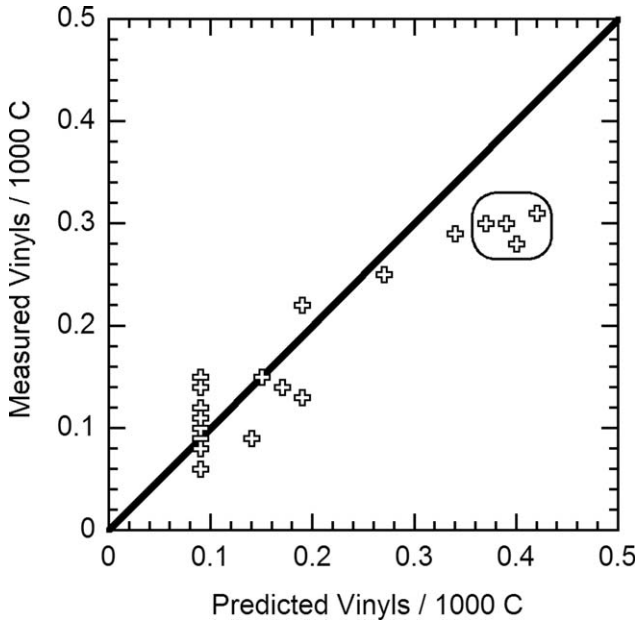


**Figure 7. Prediction of the number vinyl groups per 1000 C.**

Line: best possible agreement between experimental measurements and model predictions. Points' $x$ coordinates: calculated number of vinyl groups via Eq. 13 using $r = 2.85$, $r_{13} = 3.75$, $r_{12} = 7.5$, and data from Table 3. Points' $y$ coordinates: FTIR measurements (Table 4). Points inside the circle correspond to samples with more than 3000 ppm of incorporated decadiene.

branches produced by the incorporation of macromonomers generated via $\beta$-hydride elimination. The scattering of PDI values at low degrees of crosslinking may be caused by precision limitations in GPC measurements, and variations in the amount of $Y$ long-chain branches across the samples.

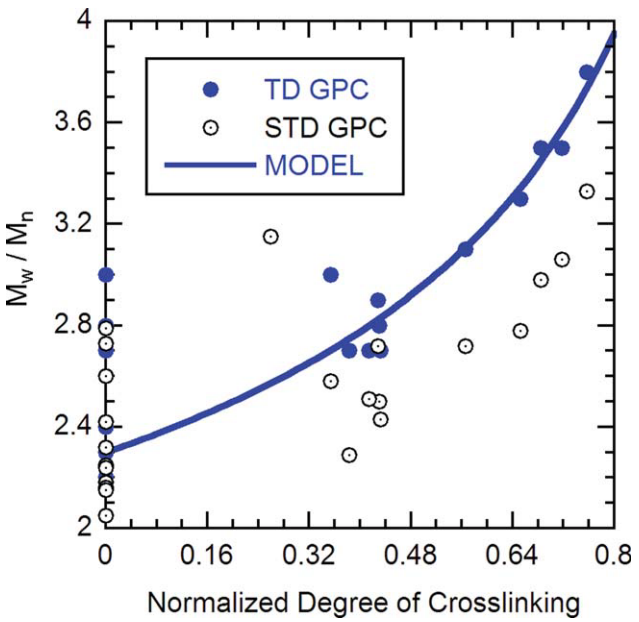


**Figure 6. PDI predictions.**

Line: Eq. 6—rescaled to give a PDI of 2.3 at $X = 0$. Points' $x$ coordinates: calculated values via Eq. 16, using $r = 2.85$, $r_{13} = 3.75$, $r_{12} = 7.5$, and data from Table 3. Points' $y$ coordinates: TD-GPC measurements (Table 4). [Color figure can be viewed in the online issue, which is available at www.interscience.wiley.com.]

The PDI values measured by TD-GPC and the PDIs predicted by the model are normally higher than the values measured by conventional (infrared-based) GPC, presumably because conventional GPC underestimates the molecular weight of branched species. The underestimation of molecular weights occurs because conventional GPC assigns molecular weights based on hydrodynamic volume, and branched polymer chains have smaller hydrodynamic volumes than linear counterparts of the same molecular weight.[18]

Figure 7 compares the model predictions for the number of vinyl groups with FTIR measurements. The number of vinyl groups generated by decadiene addition is estimated from Eq. 13. Vinyl groups formed by $\beta$-hydride elimination are simply added to the predicted decadiene contribution. On average, 0.09 vinyls / 1000 C were detected in samples with no decadiene. Thus, 0.09 vinyls / 1000 C were added to Eq. 13 results. The agreement between model predictions and FTIR measurements, however, is not satisfactory. The model overestimates the number of vinyl groups for samples with more than 3000 ppm of incorporated decadiene (compare Tables 4 and 5). A large number of additional $H$ branches would be needed to explain the relatively low number of vinyl groups detected by FTIR measurements. The value of $r$ would need to be as low as 0.7 to fit the vinyl data, suggesting that dangling double bonds are more reactive than their unattached counterparts (an unphysical result). In addition, for $r = 0.7$, run 2 and runs 20 through 25 would be predicted to be well above the onset of gelation, a result

not supported by the chromatographic data and in contradiction with the smooth process operation observed for most of these runs (only run 25 showed signs of fouling).

If the FTIR data are correct, vinyl groups must be consumed in reactions that do not form *H* branches or in reactions that form *H* branches without impacting the polydispersity and the average molecular weight of the system. *H* branches may have a small effect on polydispersity and average molecular weight when they join very small polymer chains or when they join polymer chains at the ends. For practical purposes, however, a high value of *r* captures all the decadiene inefficiencies (whatever their source may be), and the simple model developed here is useful for the prediction of critical diene concentrations and expected polymer properties (other than the number of vinyl groups).

An additional and crucial test for the model is whether it can predict (and prevent) the onset of fouling. In our experiments, no fouling occurred when the decadiene concentration remained below 70% of the calculated critical concentration. In the last runs, where an experimental determination of the fouling decadiene concentration was attempted, fouling was minor and it did not cause major plant disturbances.

The onset of fouling was indicated by abnormal viscosity readings from the Micro-Motion meter located at the reactor outlet. Polymer buildup reduced the meter's effective pipe diameter and the viscosity estimate increased significantly (see Figure 8). Relatively high viscosity readings continued after standard cleaning efforts (high-viscosity scrub runs, hot-solvent flushes). The decadiene experiments, however, did not affect the operation of the plant. Fouling was limited to the Micro-Motion meter, and the shift in viscosity estimates remained constant (after cleaning runs), allowing a consistent reactor control in subsequent experiments. The viscosity readings returned to normal values only after the meter was replaced, 3 months later. Postmortem inspection of the meter revealed small amounts of polymer residue trapped inside the instrument, but it was not possible to obtain a large enough sample for analysis.

**Table 5. Model Predictions**

| Sample | $\rho$, g/cm$^3$ | $M_w$, kg/mol | PDI | Vinyls/ 1000 C | $C_{10}$ inc. (ppm) | $X$ (%) |
|---|---|---|---|---|---|---|
| 1 | 0.962 | 48 | 2.3 | 0.09 | 0 | 0 |
| 2 | 0.960 | | 2.8 | 0.27 | 2141 | 43 |
| 3 | 0.962 | | 2.3 | 0.09 | 0 | 0 |
| 4 | 0.960 | 64 | 2.3 | 0.09 | 0 | 0 |
| 5 | 0.958 | 80 | 2.7 | 0.19 | 1192 | 35 |
| 6 | 0.959 | 67 | 2.3 | 0.09 | 0 | 0 |
| 7 | 0.959 | 61 | 2.3 | 0.09 | 0 | 0 |
| 8 | 0.958 | 76 | 2.7 | 0.14 | 743 | 38 |
| 9 | 0.959 | | 2.3 | 0.09 | 0 | 0 |
| 10 | 0.962 | 44 | 2.3 | 0.09 | 0 | 0 |
| 11 | 0.959 | 59 | 2.8 | 0.17 | 1116 | 43 |
| 12 | 0.961 | 47 | 2.3 | 0.09 | 0 | 0 |
| 13 | 0.876 | 67 | 2.3 | 0.09 | 0 | 0 |
| 14 | 0.875 | 80 | 2.6 | 0.19 | 1170 | 26 |
| 15 | 0.877 | 71 | 2.3 | 0.09 | 0 | 0 |
| 16 | 0.920 | 62 | 2.3 | 0.09 | 0 | 0 |
| 17 | 0.919 | 80 | 2.8 | 0.15 | 796 | 41 |
| 18 | 0.921 | 63 | 2.3 | 0.09 | 0 | 0 |
| 19 | 0.921 | 48 | 2.3 | 0.09 | 0 | 0 |
| 20 | 0.919 | 63 | 2.8 | 0.27 | 2145 | 43 |
| 21 | 0.919 | 70 | 3.1 | 0.34 | 2880 | 57 |
| 22 | 0.918 | 76 | 3.3 | 0.37 | 3257 | 65 |
| 23 | 0.918 | 79 | 3.4 | 0.39 | 3429 | 68 |
| 24 | 0.918 | 82 | 3.6 | 0.40 | 3609 | 72 |
| 25 | 0.918 | 87 | 3.7 | 0.42 | 3789 | 76 |

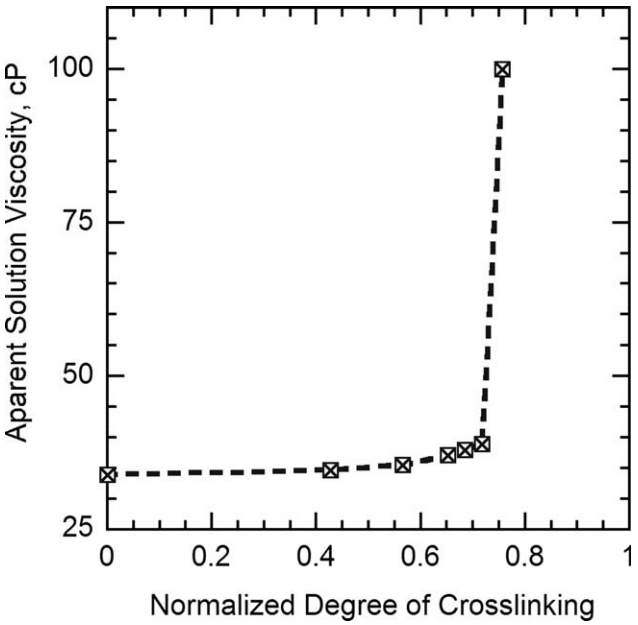


**Figure 8. Onset of fouling.**

Points: reactor solution viscosity reading for runs 19 through 25 as a function of the normalized degree of crosslinking. The dashed line is to guide the eye.

According to the chromatographic data (and the theory), only ~75% of the critical decadiene concentration for gelation was reached. The weight-average molecular weight almost doubled (Figure 5), but a four-fold increase is predicted at the onset of gelation. The PDI approached 4 (Figure 6), but a value of 7 is expected at gelation. Assuming that fouling was not due to other factors, the experimental results indicate that decadiene can cause localized fouling before system-wide gelation. This is expected, because temperature and concentration gradients are unavoidable in real systems, and highly crosslinked material can be produced even when the average decadiene concentration is low. Nevertheless, the likelihood of synthesizing highly crosslinked material increases significantly as the average bulk concentration approaches the critical concentration for gelation. In our experiments, the model was able to predict a fouling-free operation boundary. No unintended fouling occurred during 2 weeks of continuous operation, and fouling only occurred when we deliberately approached the predicted critical concentration for gelation.

## Conclusions

We have developed a simple model to predict a gel-free operation boundary in continuous olefin-diene copolymerizations. Continuous runs in a small industrial reactor have been conducted to validate the model and to characterize the response of a constrained-geometry catalyst. The experimental results indicate that the unattached 1,9-decadiene double bonds are as reactive as those of 1-octene, but the decadiene double bonds attached to polymer chains appear to be less

reactive than their unattached counterparts. The difference in reactivity reduces the LCB efficiency of the decadiene molecule, and it makes the onset of gelation more abrupt than it would be in an equal reactivity case.

Overall, the model proposed here agrees well with chromatographic, density, and mass-balance data, and the model is useful in preventing reactor fouling. Although in practice, fouling can occur for many reasons and the onset of fouling may occur before system-wide gelation, the model provides valuable guidance. In our experiments, no fouling occurred when decadiene concentrations were kept at or below 70% of the calculated critical concentration for gelation.

## Acknowledgments

This work could not have been completed without the support of the analytical and pilot-plant teams of the Dow Chemical Company. The authors specially thank Dan Baugh for thorough NMR experiments, and Mike Turner, Sarat Munjal, and the reviewer for useful comments.

## Literature Cited

1. Gabriel C, Munstedt H. Influence of long-chain branches in polyethylenes on linear viscoelastic flow properties in shear. *Rheol Acta*. 2002;41:232–244.
2. Yan D, Wang WJ, Zhu S. Effect of long chain branching on rheological properties of metallocene polyethylene. *Polymer*. 1999;40:1737–1744.
3. Dekmezian AH, Weng W, Garcia-Franco CA, Markel EJ. Melt strength of blends of linear low density polyethylene and comb polymers. *Polymer*. 2004;45:5635–5640.
4. Bortner MJ, Doerpinghaus PJ, Baird DG. Effects of sparse long chain branching on the spinning stability of LLDPEs. *Int Polym Process*. 2004;19:236–243.
5. Lai SY, Wilson JR, Knight GW, Stevens JC, Chum PWS, inventors; The Dow Chemical Company, assignee. Elastic substantially linear olefin polymers. US patent 5,272,236. December 21, 1993.
6. Kolodka E, Wang WJ, Charpentier PA, Zhu S, Hamielec AE. Long-chain branching in slurry polymerization of ethylene with zirconocene dichloride/modified methylaluminoxane. *Polymer*. 2000;41:3985–3991.
7. Pietikäinen P, Väänänen T, Seppälä JV. Copolymerization of ethylene and non-conjugated dienes with $Cp_2ZrCl_2$/MAO catalyst system. *Eur Polym J*. 1999;35:1047–1055.
8. Uozumi T, Tian G, Ahn CH, Jin J, Tsubaki S, Sano T, Soga K. Synthesis of functionalized alternating olefin copolymer and modification to graft copolymer by hydrosilylation. *J Polym Sci Part A*. 2000;38:1844–1847.
9. Hild G, Rempp P. Mechanism of network formation by radical copolymerization. *Pure Appl Chem*. 1981;53:1541–1556.
10. Nele M, Soares JBP, Pinto JC. Evolution of molecular weight and long chain branch distributions in olefin-diene copolymerization. *Macromol Theory Simul*. 2003;12:582–592.
11. Dias RCS, Costa MRPFN. Branching and crosslinking in coordination terpolymerizations. *Macromol React Eng*. 2007;1:440–467.
12. ver Strate G, Cozewith C, Graessley WW. Branching by copolymerization of monovinyl and divinyl monomers in continuous-flow stirred reactors. *J Appl Polym Sci*. 1980;25:59–62.
13. Cozewith C, Teymour F. Polymer cross-linking in post-gel region for continuous and batch reactors. *AIChE J*. 1998;44:722–732.
14. Mayo FR, Lewis FM. Copolymerization. I. A basis for comparing the behavior of monomers in copolymerization; the copolymerization of styrene and methyl methacrylate. *J Am Chem Soc*. 1944;66:1594–1601.
15. Galimberti M, Mascellani N, Piemontesi F, Camurati I. Random ethane/propene copolymerization from a catalyst system based on a "constrained geometry" half-sandwich complex. *Macromol Rapid Commun*. 1999;20:214–218.
16. Xu G, Ruckenstein E. Ethylene copolymerization with 1-octene using a 2-methylbenz[e]indenyl-based ansa-monocyclopentadienylamido complex and methylaluminoxanes catalyst. *Macromolecules*. 1998;31:4724–4729.
17. Soga K, Uozumi T, Nakamura S, Toneri T, Teranishi T, Sano T, Arai T, Shiono T. Structures of polyethylene and copolymers of ethylene with 1-octene and oligoethylene produced with the $Cp_2ZrCl_2$ and $[(C_5Me_4)SiMe_2N(t\text{-}Bu)]TiCl_2$ catalysts. *Macromol Chem Phys*. 1996;197:4237–4251.
18. Williams T, Ward IM. The construction of a polyethylene calibration curve for gel permeation chromatography using polystyrene standards. *J Polym Sci B, Polym Let*. 1968;6:621–624.

*Manuscript received Feb. 18, 2009, and revision received July 30, 2009.*